

Quantum battery optimized by parametric amplification

Fang-Mei Yang,^{1,2} Jun-Hong An,^{3,2} and Fu-Quan Dou^{1,2,*}

¹College of Physics and Electronic Engineering, Northwest Normal University, Lanzhou, 730070, China

²Gansu Provincial Research Center for Basic Disciplines of Quantum Physics, Lanzhou, 730000, China

³Key Laboratory of Quantum Theory and Applications of MoE, Lanzhou Center for Theoretical Physics, and Key Laboratory of Theoretical Physics of Gansu Province, Lanzhou University, Lanzhou 730000, China

The parametric amplification enabled by two-photon driving constitutes a versatile platform for advanced quantum technologies. We present an optimized scheme for implementing quantum batteries (QBs) based on a superconducting circuit system, where a two-photon-driven LC resonator serves as the charger and an array of transmon qubits functions as the battery. Our results show that two-photon parametric driving exponentially enhances the effective cavity-qubit coupling, which in turn gives rise to near-degenerate energy-level structures and highly entangled quantum states. This significantly enhances the charging power and enables rapid energy transfer from the charger to the battery. Moreover, the engineered squeezed cavity mode and the associated quantum correlations effectively suppress environmentally induced decoherence, thereby delaying energy leakage and facilitating stable energy storage. The proposed scheme remains robust against practical experimental imperfections, such as parameter disorder and environmental noise, preserving its performance advantages. The work provides a feasible platform for realizing high-power, high-stability QBs and highlights the potential of parametric control in quantum energy technologies.

I. INTRODUCTION

Quantum batteries (QBs) are emerging energy storage devices based on nonequilibrium quantum thermodynamics, consisting of quantum systems with discrete energy levels that are excited to temporarily store energy [1–3]. Their core mechanism relies on multipartite quantum correlations to realize superlinear scaling in charging power, thereby exhibiting a quantum advantage over classical linear scaling [4–13]. This advantage has motivated extensive studies, mainly devoted to model innovation [14–24], performance optimization [25–39], and experimental validation [40–48]. The coupling strength between the battery and the charger directly determines the charging power and serves as the key tuning parameter for realizing quantum advantage [2, 49, 50]. In practice, overly weak coupling restricts the charging rate, whereas excessively strong coupling both exacerbates decoherence and poses experimental difficulties. Therefore, optimizing the trade-off between coupling strength and decoherence, together with developing precise control techniques, constitutes a critical challenge for current experimental research on QBs.

The strong coupling regime is essential for observing coherent quantum dynamics between light and matter [50]. Significant progress in nanofabrication and quantum control has enabled the realization of strong coupling across diverse platforms, including superconducting circuits, semiconductor quantum dots, and solid-state spin systems [51–56]. In 2016, two independent experiments attained a qualitative jump in the light-matter interaction strength, pushing the boundaries into the nonperturbative ultra-strong coupling domain by using Josephson junctions as coupling elements [57–62]. Subsequently,

the deep-strong coupling regime has been experimentally realized in both superconducting circuits and in two-dimensional electron gases coupled to terahertz metamaterial resonators [63, 64]. In two regimes, where light-matter interactions approach or exceed the bare frequencies of the uncoupled systems, counter-rotating terms in the Hamiltonian become nonnegligible, leading to novel dynamics and entanglement properties [65–71]. Nevertheless, current implementations are generally limited by fabrication complexity, constrained tunability, and scalability challenges, which hinder the simultaneous attainment of high coupling strengths, precise dynamic control, and large-scale integration. Thus, developing generalizable approaches that do not depend on highly specialized materials or device architectures is crucial for unlocking the full potential of these extreme coupling regimes in future quantum applications.

Parametric amplification techniques, especially those based on nonlinear two-photon driving, provide a promising physical pathway to address these limitations [72–79]. These approaches utilize intrinsic nonlinearities, such as Josephson or Kerr nonlinearity, to enable frequency conversion and mode coupling, thereby inducing effective ultra-strong or deep-strong coupling dynamics in systems that are otherwise strongly coupled [79–82]. This strategy not only eliminates the dependence on specialized materials or device architectures, but also allows dynamic tuning of coupling strengths through control parameters including drive amplitude and frequency. Furthermore, two-photon parametric processes naturally generate squeezed states, which can further suppress environmental noise and enhance system coherence [79, 83, 84]. Consequently, parametric amplification via two-photon driving offers new theoretical and experimental prospects for optimizing and realizing quantum systems in the ultra-strong and deep-strong coupling regimes under flexible and controllable conditions.

* doufq@nwnu.edu.cn

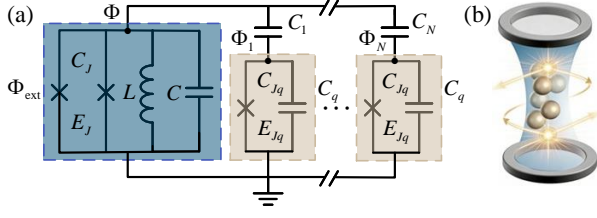


FIG. 1. (a) The schematic illustrates a superconducting circuit architecture consisting of an LC resonator, with inductance L and capacitance C , capacitively coupled to an array of N transmon qubits. Each qubit is modeled as a capacitor C_q in parallel with a Josephson junction characterized by energy E_{Jq} and capacitance C_{Jq} . The capacitive coupling is realized via the same capacitors C_j . A flux-pumped superconducting quantum interference device, formed by two Josephson junctions each with energy E_J and capacitance C_J , is threaded by an external magnetic flux Φ_{ext} and embedded in the resonator loop to provide a tunable nonlinear inductive element. When the device is driven at twice the resonator frequency, it mediates an effective parametric two-photon driving to the cavity mode, enabling controlled squeezing of the microwave field. (b) Illustration of the QB. The golden arrows represent the optimization process facilitated by two-photon driving.

In this work, we propose a superconducting quantum circuit consisting of a two-photon-driven LC resonator coupled to an array of transmon qubits, providing a physical platform for the optimization and realization of QBs. Our study focuses on the exponential enhancement of the cavity-qubit coupling via two-photon parametric amplification, elucidating its pivotal role in boosting the charging and storage properties of QBs. We explore rapid energy transfer dynamics supported by near-degenerate energy-level structures, while analyze how squeezed cavity modes and correlated quantum states suppress energy leakage during stable energy storage. By investigating the effects of parameter disorder and environmental dissipation, we further demonstrate the robustness of this scheme under realistic experimental conditions, thereby establishing a theoretical framework and a feasible pathway toward readily scalable, high-performance quantum energy storage systems.

The paper is organized as follows. A superconducting quantum circuit system is presented in Sec. II, where we derive its Hamiltonian and analyze the mechanism underlying the exponentially enhanced coupling induced by two-photon driving. In Sec. III, we construct a QB model based on this system, discuss its collective charging advantage, and examine its robustness against parameter disorder and environmental dissipation. The main results are summarized in Sec. IV. The quantum criticality and quantum fluctuation of the system is addressed in Appendix A. In Appendix B, a more generalized quantum battery model is established and an approximate bound for its charging power is derived.

II. CIRCUIT QED

We consider a superconducting quantum circuit comprising an LC resonator under two-photon driving and an ensemble of N transmon qubits, shown in Fig. 1(a). The two-photon driving is implemented via a pair of Josephson junctions connected in parallel with the resonator, generating an effective squeezing Hamiltonian for the cavity mode. This design enables the controlled enhancement of quantum fluctuations and facilitates the exploration of strong correlations in cavity quantum electrodynamics at reduced physical coupling strengths [75]. The entire circuit is described by the following Lagrangian

$$\mathcal{L} = \mathcal{L}_{\text{cavity}} + \mathcal{L}_{\text{qubits}} + \mathcal{L}_{\text{coupling}} + \mathcal{L}_{\text{squeezing}},$$

where

$$\begin{aligned} \mathcal{L}_{\text{cavity}} &= \frac{1}{2}C\dot{\Phi}^2 - \frac{1}{2L}\Phi^2, \\ \mathcal{L}_{\text{qubits}} &= \sum_{j=1}^N \left[\frac{1}{2}(C_q + C_{Jq})\dot{\Phi}_j^2 + E_{Jq} \cos\left(2\pi\frac{\Phi_j}{\Phi_0}\right) \right], \\ \mathcal{L}_{\text{coupling}} &= \sum_{j=1}^N \left[\frac{1}{2}C_j(\dot{\Phi} - \dot{\Phi}_j)^2 \right], \\ \mathcal{L}_{\text{squeezing}} &= C_J\dot{\Phi}^2 + 2E_J \cos\left(\pi\frac{\Phi_{\text{ext}}}{\Phi_0}\right) \cos\left(2\pi\frac{\Phi}{\Phi_0}\right). \end{aligned}$$

Here, the parameters Φ and Φ_j denote the magnetic fluxes at the respective nodes, $\Phi_0 = h/2e$ is the flux quantum and $\Phi_{\text{ext}} = \Phi_{dc} + \delta\Phi \cos(\omega_p t)$ is the external flux with the parametric drive frequency ω_p . The large Josephson energy restricts the phase to small fluctuations near zero, which justifies the expansion of the cosine terms in the Lagrangian to fourth order [85]. The classical Hamiltonian is subsequently derived through the Legendre transformation

$$\begin{aligned} H &\approx \frac{1}{2C_c}Q^2 + \frac{1}{2L_c}\Phi^2 - \frac{\lambda_0}{\Phi_0^2} \cos(\omega_p t) \Phi^2 \\ &+ \sum_{j=1}^N \left[\frac{1}{2C_q}Q_j^2 + \frac{1}{2L_q}\Phi_j^2 - \frac{C_j}{C_c C_q}QQ_j \right], \end{aligned} \quad (1)$$

where $Q_k = \partial\mathcal{L}/\partial\Phi_k$ and $\lambda_0 = 4E_J\pi^3\frac{\delta\Phi}{\Phi_0} \sin(\pi\frac{\Phi_{dc}}{\Phi_0})$, with k either empty or an index j .

In the weak-coupling regime, the cavity and the qubits can be quantized independently. Equation (1) is thus quantized by requesting the canonical commutation relation $[\Phi_k, Q_k] = i\hbar$. The annihilation operators are

$$a = \frac{\Phi}{\sqrt{2\hbar Z_c}} + i\sqrt{\frac{Z_c}{2\hbar}}Q, \quad b_j = \frac{\Phi_j}{\sqrt{2\hbar Z_q}} + i\sqrt{\frac{Z_q}{2\hbar}}Q_j. \quad (2)$$

From these relations, the quantized Hamiltonian is ex-

pressed as

$$H = \hbar\omega_c a^\dagger a - \frac{\hbar\lambda_0}{2C_c\Phi_0^2\omega_c} \cos(\omega_p t) (a + a^\dagger)^2 + \sum_{j=1}^N \left[\hbar\omega_q b_j^\dagger b_j - \frac{\hbar C_j}{2\omega_c\omega_q} (ab_j^\dagger + a^\dagger b_j) \right], \quad (3)$$

with the impedance $Z_{k_1} = \sqrt{L_{k_1}/C_{k_1}}$ and the frequency $\omega_{k_1} = 1/\sqrt{L_{k_1}C_{k_1}}$ for $k_1 = c, q$. In a regime where the anharmonicity of the transmon is large, we can reduce the transmon to a two-level system [86]. The Hamiltonian is truncated to two lowest levels and written as

$$H = \hbar\omega_c a^\dagger a - \hbar\lambda \cos(\omega_p t) (a + a^\dagger)^2 + \hbar\omega_q J_z - \hbar g (aJ_+ + a^\dagger J_-), \quad (4)$$

the components of a collective spin operator are defined in terms of the Pauli operators as $J_{x,y,z} = \sum_{j=1}^N \sigma_{x,y,z}^j/2$. Here, $g = C_j/(\omega_c\omega_q)$ and $\lambda = \lambda_0/(2C_c\Phi_0^2\omega_c)$ denote the cavity-qubit coupling strength and the parametric drive amplitude, respectively.

We then move the time-dependent Hamiltonian (4) into a frame rotating at half the parametric drive frequency ω_p , with the unitary operator chosen as $U_p = e^{-i\omega_p t(a^\dagger a + J_z)/2}$. The Hamiltonian becomes

$$H_p = \hbar\delta_c a^\dagger a + \hbar\delta_q J_z - \hbar g (aJ_+ + a^\dagger J_-) - \frac{\hbar\lambda}{2} (a^2 + a^{\dagger 2}), \quad (5)$$

where the cavity and qubit detunings are given by $\delta_{c/q} = \omega_{c/q} - \omega_p/2$. By a unitary transformation $U_s = e^{\tau/2(a^{\dagger 2} - a^2)}$, with a squeezing parameter r defined as $\tanh(2r) = \lambda/\delta_c$, Eq. (5) is recast into

$$H_s = \hbar\delta_c \operatorname{sech}(2r) a^\dagger a + \hbar\delta_q J_z - \frac{\hbar g}{2} e^r (a^\dagger + a) \times (J_+ + J_-) + \frac{\hbar g}{2} e^{-r} (a^\dagger - a) (J_+ - J_-). \quad (6)$$

The Hamiltonian takes the form of a generalized Dicke model with an additional term whose coupling strength decreases exponentially. Under strong parametric driving, the system becomes intrinsically equivalent to the standard Dicke model, characterized by an effective cavity detuning $\tilde{\delta}_c = \delta_c \operatorname{sech}(2r)$ and an enhanced coupling strength $\tilde{g} = ge^r/2$. The resulting effective critical coupling is given by $g_c = \sqrt{\tilde{\delta}_c \tilde{\delta}_q \operatorname{sech}(2r)}/2$, see Appendix A for the derivation. The two-photon driving exponentially amplifies the cavity mode fluctuations, simultaneously increasing the effective light-matter coupling and reducing the effective critical coupling. Thus, the quantum phase transition occurs at a value significantly lower than the bare coupling strength.

We take into account the resonance case $\delta_q = \delta_c$. We find that the two-photon driving can shift the quantum phase transition threshold from the ultra-strong coupling regime $g/\delta_c = 0.5$ without driving to the strong coupling

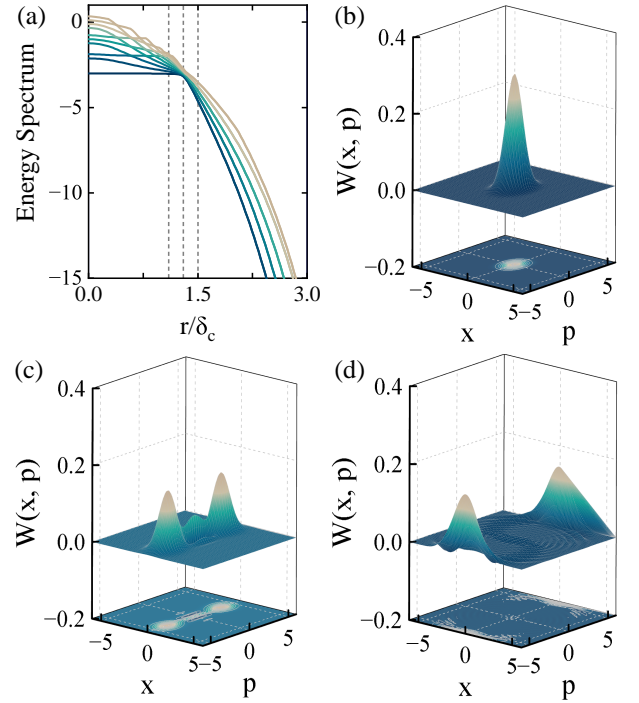


FIG. 2. (a) The first ten energy levels versus the squeezing parameter, with the number of qubits fixed at $N = 6$. (b-d) The ground-state Wigner functions at different squeezing parameters $r/\delta_c = 1.1, 1.3, 1.5$. Other parameters are $\delta_q/\delta_c = 1$, and $g/\delta_c = 0.05$.

regime $g/\delta_c = 0.05$ at a squeezing parameter $r/\delta_c \approx 1.22$. Figure 2(a) shows the variation of the energy spectrum with the squeezing parameter. Increasing this parameter drives the system from a non-degenerate strong-coupling regime to an ultra-strong-coupling regime with pairs of near-degenerate energy-level structures, concurrent with the normal-to-superradiant phase transition. In Figs. 2(b)-2(c), we introduce the Wigner quasi-probability distribution $W(x, p) = \frac{1}{\pi\hbar} \int_{-\infty}^{+\infty} \langle x + y | \rho_g | x - y \rangle e^{-2ipy/\hbar} dy$ to probe quantum features, where ρ_g is the ground-state density matrix of the cavity mode [87]. Across the normal-to-superradiant phase transition, the ground state evolves from a separable vacuum state into a quantum state with nonclassical entanglement. The corresponding Wigner function exhibits a pronounced bimodal structure with negative-value regions, indicating that significant quantum correlations and squeezing effects emerge during the quantum phase transition. Overall, parametric amplification enabled by two-photon driving provides enhanced coupling strength and macroscopic entangled states, forming a versatile platform for advanced quantum technologies. The resulting squeezed cavity field facilitates quantum metrology beyond the standard quantum limit [88, 89], while the exponentially amplified coupling underpins strongly correlated states that are indispensable for high-power, high-fidelity quantum devices, such as QBs.

III. QB MODEL AND ITS CHARGING ADVANTAGES

As illustrated in Fig. 1(b), our model features a battery $H_b = \hbar\omega_q J_z$ consisting of N transmon qubits and a charger $H_c = \hbar\omega_c a^\dagger a$ realized by a superconducting cavity. Moving beyond idealizations, real-world devices are inherently open systems susceptible to environmental noise. Therefore, the charging performance is quantified here under two dominant experimental decoherence channels. The charging dynamics is described by the following Lindblad master equation $\frac{d\rho}{dt} = -\frac{i}{\hbar}[H, \rho] + (\kappa\mathbb{L}_{a,a^\dagger} + \gamma\mathbb{L}_{J_-, J_+})\rho$, where the superoperator is defined as $\mathbb{L}_{o,p} \cdot = o \cdot p - \{p o, \cdot\}/2$, κ is the photon-loss rate from the cavity, and γ is the collective relaxation rate of the qubit ensemble. Under the squeezed transformation $\rho_s = U_s^\dagger \rho U_s$, the dynamical equation retains the form

$$\frac{d\rho_s}{dt} = -\frac{i}{\hbar}[H_s, \rho_s] + (\kappa\mathbb{L}_{a_s, a_s^\dagger} + \gamma\mathbb{L}_{J_-, J_+})\rho_s, \quad (7)$$

where the annihilation operator becomes $a_s = U_s^\dagger a U_s = a \cosh r + a^\dagger \sinh r$. The explicit form of $\mathbb{L}_{a_s, a_s^\dagger} \rho_s$ as

$$\mathbb{L}_{a_s, a_s^\dagger} \rho_s = [\cosh^2 r \mathbb{L}_{a, a^\dagger} + \sinh^2 r \mathbb{L}_{a^\dagger, a} + \cosh r \sinh r (\mathbb{L}_{a, a} + \mathbb{L}_{a^\dagger, a^\dagger})] \rho_s, \quad (8)$$

reveals that in the squeezed frame, the single-photon loss term from the cavity is amplified, while additional gain-type and two-photon correlated dissipators emerge. This redistribution of environmental noise across phase space enables dynamical squeezing: quantum fluctuations are suppressed in one quadrature and amplified in the orthogonal one [90, 91]. Thus, the two-photon driving effectively reshapes dissipation to facilitate noise suppression and stabilize nonclassical states.

The system is initialized with the cavity in an n -photon Fock state and the qubits in their collective ground state. The total initial state is a product state given by

$$|\Psi(0)\rangle = |n\rangle \otimes \underbrace{|G, \dots, G\rangle}_N = |n; N/2, -N/2\rangle. \quad (9)$$

The numerical solution of the Dicke model requires imposing a finite photon-number cutoff n_{ph} , since photon number is not conserved and the Hilbert space is unbounded in principle. In simulations, we set the initial photon number to $n = 2N$ and the cutoff to $n_{ph} = 4N+1$, which provides numerically stable, scalable results consistent with established methods [9, 49, 92].

The charging performance is quantified by two figures of merit: the energy stored in the battery

$$E(t) = \text{Tr}[H_b \rho_s(t)] - \text{Tr}[H_b \rho_s(0)], \quad (10)$$

and the average charging power

$$P(t) = E(t)/t. \quad (11)$$

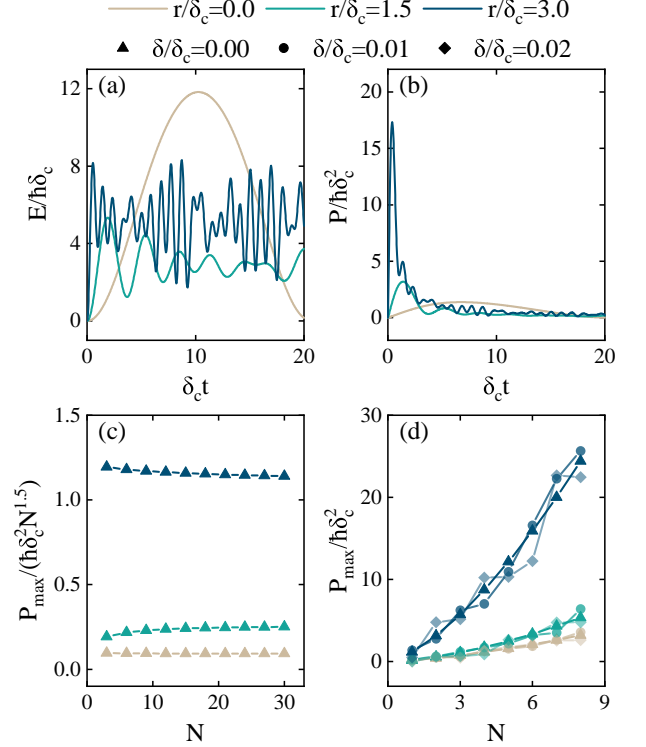


FIG. 3. Closed-system charging performance. (a) Time evolution of the stored energy and (b) charging power for different squeezing parameters $r/\delta_c = 0.0, 1.5, 3.0$. (c) Scaling of the maximum charging power with the number of qubits for the homogeneous case $\delta/\delta_c = 0$, normalized by the collective charging advantage $N^{1.5}$ of the standard Dicke model. (d) Same scaling for the inhomogeneous case $\delta/\delta_c \neq 0$, where static disorder is applied to both qubit frequencies and qubit-cavity coupling strengths. Other parameters are the same as in Fig. 2.

Additionally, the maximal energy in the closed system, the stable energy in the open system, and the maximal power attainable at any time are respectively defined as

$$E_{\max} = \max(E), \quad E_{\text{sta}} = E(\infty), \quad P_{\max} = \max(P).$$

In the closed-system scenario without cavity dissipation and qubit decoherence, Figs. 3(a) and 3(b) show the time evolution of the stored energy and charging power under varying squeezing parameters. The squeezing effect induced by two-photon driving enhances the effective charger-battery coupling but simultaneously makes the counter-rotating terms nonnegligible. These terms break the conservation of total excitation number and introduce virtual-photon-induced quantum fluctuations, preventing the battery from reaching the fully charged state. Nonetheless, the squeezing effect accelerates energy transfer from the charger to the battery, substantially increasing the charging power. Figure 3(c) displays the scaling of the maximum charging power with the number of qubits. The battery retains the collective charging advantage of the standard Dicke model, with the

maximum power following the scaling law $P_{\max} = \alpha N^\beta$ and the scaling exponent $\beta = 1.5$ [49]. Compared to the case without two-photon driving, the coefficient α increases by a factor of 12.5 at a squeezing parameter $r/\delta_c = 3$, i.e., $P_{\max}(r/\delta_c = 3)/P_{\max}(r/\delta_c = 0) \approx 12.5$, and further enhancement can be achieved by increasing either the squeezing parameter or the number of charger modes shown in Appendix B.

In practical implementations, inhomogeneity in qubit frequencies and coupling strengths is unavoidable, especially in superconducting circuits where identical qubits are extremely challenging to realize. To evaluate the experimental feasibility of this scheme, we introduce static disorder drawn from a uniform distribution, setting the frequency of the j th qubit as $\omega_j = \omega_q + \epsilon_j$ and its coupling strength to the cavity mode as $g_j = g + \eta_j$, where $\epsilon_j, \eta_j \in [-\delta, \delta]$ are independent random variables. Numerical results presented in Fig. 3(d) demonstrate that even when the inhomogeneous broadening is on the same order as the bare coupling strength, the exponentially enhanced coupling can effectively sustain the dominance of collective charging effects, allowing the battery to maintain high-power charging performance with weak sensitivity to parameter perturbations. This robustness not only verifies the strong tolerance of the scheme to non-ideal experimental conditions but also reveals a feasible pathway to overcome inherent parameter dispersion in solid-state systems via quantum control methods.

Under dissipative and decoherence conditions, the battery evolves into a steady state with finite stored energy for $r/\delta_c \neq 0$, as shown in Fig. 4(a). This behavior originates from two synergistic mechanisms: dark-state protection and environmental modification. The dark states of the many-body system satisfy $J_-|\text{dark}\rangle = 0$, where quantum interference cancels collective dipole radiation, rendering these states immune to decay via the collective relaxation channel $\gamma \mathbb{L}_{J_-, J_+}$ [93–95]. Meanwhile, the squeezing effect modifies the environmental noise shown in Eq. (8), where the $\sinh^2 r \mathbb{L}_{a^\dagger, a}$ term converts vacuum fluctuations into effective thermal excitations, effectively endowing the zero-temperature environment with a non-zero temperature in the squeezed frame. The resulting dynamic balance between energy injection and dissipation drives the battery into a steady state with finite stored energy. As shown in Fig. 4(b), the charging power retains the collective charging advantage of the closed system, indicating that dark-state protection and squeezing-enhanced coupling jointly preserve many-body cooperative effects. Figures 4(c) and 4(d) further demonstrate that even in the critically damped and overdamped regimes, where the dissipation rate approaches or exceeds the coupling strength, the battery sustains a steady state with non-zero stored energy and its associated quantum advantage.

The impact of two-photon driving exhibits a distinct trade-off depending on whether the system is closed or open. In the closed system, the enhanced charging power comes at the cost of a slight reduction in the maximum

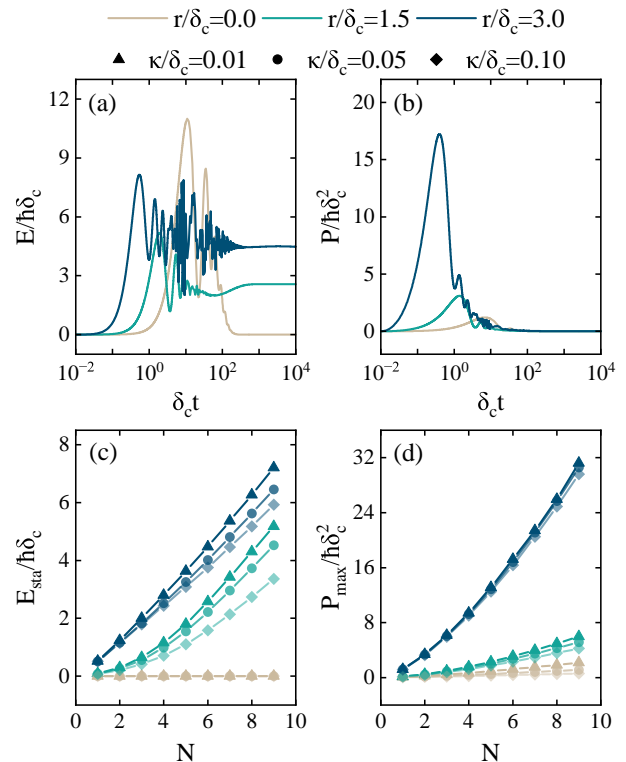


FIG. 4. Open-system charging performance. (a) Time evolution of the stored energy and (b) charging power for squeezing parameters $r/\delta_c = 0.0, 1.5, 3.0$, with fixed dissipation rates $\kappa/\delta_c = \gamma/\delta_c = 0.01$. (c) Scaling of the steady-state energy and (d) maximum charging power with the number of qubits for dissipation rates $\kappa/\delta_c = \gamma/\delta_c = 0.01, 0.05$, and 0.10 , representing the underdamped, critically damped, and overdamped regimes, respectively. All other parameters are identical to those in Fig. 2.

stored energy, as counter-rotating terms break excitation number conservation. In the open system, this trade-off yields an advantage: two-photon driving not only maintains high-power charging but also achieves stable energy storage via dark-state protection and squeezing-induced effective thermal excitation. Thus, the two-photon driving scheme exhibits dual superiority: it simultaneously improves charging and storage properties while remaining robust against parameter disorder and environmental noise. This sets a theoretical foundation for the practical application of QBs in imperfect experimental environments.

IV. CONCLUSIONS

In summary, we proposed a superconducting quantum circuit composed of a two-photon-driven LC resonator coupled to an array of transmon qubits, offering new possibilities for the optimization and realization of multipartite QBs. In such system, two-photon driving exponentially enhances the cavity-qubit coupling strength, which

in turn induces near-degenerate energy-level structures and highly entangled quantum states. This significantly enhances the charging power and enables rapid energy transfer between the charger and battery. Moreover, the squeezed cavity mode and the quantum correlations reflected in the bimodal Wigner function contribute to coherence protection and decoherence suppression during stable energy storage. We further demonstrated the robustness of the scheme under practical experimental imperfections, including parameter disorder and environmental noise, confirming that the charging and energy storage advantages remain well preserved. This work provides a feasible theoretical framework and an implementation platform for developing high-power, high-stability quantum energy storage devices, and also lays a foundation for the further application of parametric control in quantum information processing and microscopic quantum energy systems.

ACKNOWLEDGMENTS

The work is supported by the National Natural Science Foundation of China (Grant No. 12475026) and the Natural Science Foundation of Gansu Province (No. 25JRRA799). J.H.A. is supported by the National Natural Science Foundation of China (Grants No. 12275109, No. 92576202, and No. 12247101), the Quantum Science and Technology-National Science and Technology Major Project (Grant No. 2023ZD0300904), the Gansu Science and Technology Leading Talent Program (Grant No. 26RCKA011), and the Fundamental Research Funds for the Central Universities (Grant No. lzujbky-2025-jdzx07).

DATA AVAILABILITY

The data that support the findings of this article are not publicly available. The data are available from the authors upon reasonable request.

Appendix A: Quantum criticality and quantum fluctuation

Under strong parametric driving, the system considered in this work reduces to the standard Dicke model, enabling the derivation of quantum criticality and quantum fluctuation within that framework [96, 97]. The Hamiltonian (6) is reformulated as follows

$$H = \tilde{\delta}_c a^\dagger a + \delta_q J_z + \frac{g_e}{\sqrt{N}} (a^\dagger + a) (J_+ + J_-), \quad (\text{A1})$$

where the effective coupling strength $g_e = -\sqrt{N}\tilde{g}$. In the thermodynamic limit $N \rightarrow \infty$, the system can be treated via the Holstein-Primakoff transformation, which maps

the spin operators onto bosonic ones: $J_z = c^\dagger c - N/2$ and $J_+ = c^\dagger \sqrt{N - c^\dagger c} \approx \sqrt{N}c^\dagger$. Expanding to leading order in $1/N$ and keeping terms up to quadratic order, the Hamiltonian linearizes to

$$H \approx \tilde{\delta}_c a^\dagger a + \delta_q c^\dagger c + g_e (a^\dagger + a) (c^\dagger + c). \quad (\text{A2})$$

The initial state $|\Psi(0)\rangle = |n\rangle \otimes |j, -j\rangle = |n\rangle \otimes |0\rangle$, where $|n\rangle$ denotes a Fock state of the photon mode (with $n = 0$ for the vacuum) and $|0\rangle$ is the bosonic vacuum for the qubit ensemble in the Holstein-Primakoff representation.

To determine the critical coupling condition between two bosonic modes, the position and momentum operators are expressed in terms of creation and annihilation operators: $x_a = (a + a^\dagger)/\sqrt{2}$, $p_a = i(a^\dagger - a)/\sqrt{2}$, $x_c = (c + c^\dagger)/\sqrt{2}$, $p_c = i(c^\dagger - c)/\sqrt{2}$. The Hamiltonian becomes $H = \tilde{\delta}_c (p_a^2 + x_a^2)/2 + \delta_q (p_c^2 + x_c^2)/2 + 2g_e x_a x_c$. To analyze the stability of the system, the system is cast in matrix form

$$H = \frac{1}{2} \begin{pmatrix} p_a & p_c \end{pmatrix} \begin{pmatrix} \tilde{\delta}_c & 0 \\ 0 & \delta_q \end{pmatrix} \begin{pmatrix} p_a \\ p_c \end{pmatrix} + \frac{1}{2} \begin{pmatrix} x_a & x_c \end{pmatrix} \begin{pmatrix} \tilde{\delta}_c & 2g_e \\ 2g_e & \delta_q \end{pmatrix} \begin{pmatrix} x_a \\ x_c \end{pmatrix}, \quad (\text{A3})$$

which separates the contributions from position and momentum operators. The stability of the system requires the coefficient matrix of the potential-energy part to be positive definite, i.e., its determinant must be positive

$$\begin{vmatrix} \tilde{\delta}_c & 2g_e \\ 2g_e & \delta_q \end{vmatrix} = \tilde{\delta}_c \delta_q - 4g_e^2 > 0. \quad (\text{A4})$$

The onset of instability, which marks the quantum phase transition, occurs when the determinant vanishes. Solving for the coupling strength from $\tilde{\delta}_c \delta_q = 4g_e^2$ yields the critical value

$$|g_c| = \frac{1}{2} \sqrt{\tilde{\delta}_c \delta_q} = \frac{1}{2} \sqrt{\delta_c \delta_q \operatorname{sech}(2r)}. \quad (\text{A5})$$

The squeezing effect induced by two-photon driving both enhances the effective coupling and decreases the critical coupling, enabling the superradiant phase transition to occur at a significantly reduced coupling strength [97].

In the normal phase $|g_e| < |g_c|$, the ground state preserves the \mathbb{Z}_2 symmetry, implying $\langle a \rangle_G = 0$, $\langle c \rangle_G = 0$. The Hamiltonian expectation and variance in the initial state are evaluated as: $\langle H \rangle = \tilde{\delta}_c n$, $\langle H^2 \rangle = \tilde{\delta}_c^2 n^2 + g_e^2 (2n + 1)$, leading to the energy uncertainty

$$\Delta H = \sqrt{\langle H^2 \rangle - \langle H \rangle^2} = \frac{g_e}{2} e^r \sqrt{N(2n + 1)}. \quad (\text{A6})$$

In the superradiant phase $|g_e| > |g_c|$, the system undergoes spontaneous symmetry breaking, and both field and qubit ensemble acquire nonzero expectation values $\langle a \rangle_G = \sqrt{N}\alpha_1$, $\langle c \rangle_G = \sqrt{N}\beta_1$ [98, 99]. Introducing displacement $a = d + \sqrt{N}\alpha_1$, $c = e + \sqrt{N}\beta_1$, where the

displacement parameters are determined as [96]

$$\alpha_1 = \frac{g_e}{\sqrt{\tilde{\delta}_c \delta_q}} \sqrt{1 - \frac{g_c^2}{g_e^2}}, \quad \beta_1 = -\frac{1}{2} \sqrt{\frac{\tilde{\delta}_c}{\delta_q}} \sqrt{1 - \frac{g_c^2}{g_e^2}}, \quad (\text{A7})$$

we can obtain an effective quadratic Hamiltonian after removing linear terms and constant shifts

$$H \approx \tilde{\delta}_c d^\dagger d + \delta_q e^\dagger e + g_e (d^\dagger + d) (e^\dagger + e). \quad (\text{A8})$$

The initial state becomes a displaced vacuum state

$$|\Psi(0)\rangle = D(-\sqrt{N}\alpha_1)|n\rangle \otimes D(-\sqrt{N}|\beta_1|)|0\rangle. \quad (\text{A9})$$

The expectation values of the energy and its square in the initial state are

$$\begin{aligned} \langle H \rangle &= \tilde{\delta}_c n + \tilde{\delta}_c \alpha^2 N + \delta_q \beta^2 N - 4g_e \alpha \beta N, \\ \langle H^2 \rangle &= \langle H \rangle^2 + \left[4g_e^2 (\alpha^2 + \beta^2) - 4g_e (\tilde{\delta}_c + \delta_q) \alpha \beta \right] N \\ &\quad + \left(2\tilde{\delta}_c^2 \alpha^2 + 8g_e^2 \beta^2 - 8g_e \tilde{\delta}_c \alpha \beta \right) n N \\ &\quad + \left(\tilde{\delta}_c^2 + 2g_e^2 \right) n + g_e^2. \end{aligned}$$

In the thermodynamic limit, the energy uncertainty tends to

$$\Delta H \approx \frac{1}{2} \sqrt{\mu e^{6r} + (\mu + \nu) e^{2r} + 2\nu(8n + 3)}, \quad (\text{A10})$$

where $\mu = N^3 g^4 / 2\delta_c \delta_q$ and $\nu = N^2 g^2$. Two-photon squeezing enhances quantum fluctuations exponentially due to its inherent nonlinearity, whereas merely increasing the initial photon number yields only linear growth in average energy and square-root growth in energy uncertainty. Hence, two-photon driving is far more efficient at enhancing quantum fluctuations than simply adding more photons.

Appendix B: Charging power bound

Compared to the lumped-parameter LC resonator, the one-dimensional transmission line cavity exhibits distributed characteristics and can be modeled as a cascade of LC circuits [100]. This architecture allows for precise control over its mode structure, vacuum fluctuations, and coupling strengths through geometric parameters such as characteristic impedance and length [100, 101]. Under the weak-coupling condition and considering an external drive field propagating along the transmission line, we derive the effective Hamiltonian for a two-photon driven transmission line cavity coupled to transmon qubits. The Hamiltonian reads

$$\begin{aligned} H &= \sum_{i=1}^m \left[\hbar \omega_c a_i^\dagger a_i - \hbar \lambda \cos(\omega_p t) (a_i + a_i^\dagger)^2 \right] \\ &\quad + \hbar \omega_q J_z - \sum_{i=1}^m \hbar g (a_i J_+ + a_i^\dagger J_-), \end{aligned} \quad (\text{B1})$$

which consists of m independent cavity modes, the two-photon driving, the free Hamiltonian of N qubits, and the coupling between cavity modes and qubits. To eliminate the explicit time dependence of the drive field and to renormalize the quantum fluctuations of the cavity field quadratures, we introduce two unitary transformations

$$U_r = \prod_{i=1}^m e^{-i \frac{\omega_p t}{2} a_i^\dagger a_i} e^{-i \frac{\omega_p t}{2} J_z}, \quad U_s = \prod_{i=1}^m e^{\frac{r}{2} (a_i^{\dagger 2} - a_i^2)},$$

and the effective Hamiltonian takes the form

$$\begin{aligned} H_s &= \sum_{i=1}^m \hbar \delta_c \operatorname{sech}(2r) a_i^\dagger a_i + \hbar \delta_q J_z \\ &\quad - \sum_{i=1}^m \frac{\hbar g}{2} e^r (a_i^\dagger + a_i) (J_+ + J_-) \\ &\quad + \sum_{i=1}^m \frac{\hbar g}{2} e^{-r} (a_i^\dagger - a_i) (J_+ - J_-). \end{aligned} \quad (\text{B2})$$

Here, the system describes a multimode cavity under two-photon driving coupled to an ensemble of qubits. Setting $m = 1$ recovers the generalized Dicke model with a correction term discussed in the main text, and further taking $r = 0$ reproduces the standard Dicke model.

We then analyze the charging power of the QB defined in this system. The average charging power is defined as the time derivative of the energy in the QB [8, 102], i.e.,

$$\begin{aligned} P(t) &= \operatorname{Tr} \left(H_b \frac{d\rho_s}{dt} \right) = -i \operatorname{Tr} (H_b [H_s, \rho_s]) \\ &= -i \operatorname{Tr} ([H_b, H_s] \rho_s) = -i \operatorname{Tr} ([H_b, H_{int} + H_{cor}] \rho_s), \end{aligned} \quad (\text{B3})$$

where H_{int} and H_{cor} correspond to the last two terms of the effective Hamiltonian (B2). In the derivation, we have used the cyclic property of the trace and the fact that H_b commutes with other terms. Using the operator norm inequality and strong parametric driving, the absolute value of the power satisfies

$$\begin{aligned} |P(t)|_{r \rightarrow \infty} &= | -i \operatorname{Tr} ([H_b, H_{int}] \cdot \rho_s) | \\ &\leq \| [H_b, H_{int}] \| \leq 2 \| H_b \| \| H_{int} \| \\ &= \frac{e^r}{2} |P(t)|_{r=0} = \frac{m e^r}{2} |P(t)|_{Dicke}. \end{aligned} \quad (\text{B4})$$

This inequality reveals that the upper bound of the maximum charging power scales exponentially with the squeezing parameter r and linearly with the number of cavity modes m . For $m = 1$ and $r = 0$, the system reduces to the standard Dicke model, with maximum power $|P(t)|_{Dicke}$ as the benchmark. For $m = 1$ and $r > 0$, the single-mode squeezed cavity enhances the power bound by a factor of $e^r/2$ compared to the Dicke model. For $m > 1$ and $r > 0$, the multimode structure further boosts the power bound by an additional factor of m , yielding $(m e^r / 2) |P(t)|_{Dicke}$. Thus, the combination of squeezing and multimode structures synergistically enhances the charging power. This suggests that using multimode

transmission line cavities with squeezed light can surpass

the power limits of conventional single-mode systems, offering a viable route toward high-performance QBs.

-
- [1] R. Alicki and M. Fannes, Entanglement boost for extractable work from ensembles of quantum batteries, *Phys. Rev. E* **87**, 042123 (2013).
- [2] F. Campaioli, S. Gherardini, J. Q. Quach, M. Polini, and G. M. Andolina, Colloquium: Quantum batteries, *Rev. Mod. Phys.* **96**, 031001 (2024).
- [3] D. Ferraro, F. Cavaliere, M. G. Genoni, G. Benenti, and M. Sassetti, Opportunities and challenges of quantum batteries, *Nat. Rev. Phys.* **8**, 115 (2026).
- [4] G. M. Andolina, M. Keck, A. Mari, V. Giovannetti, and M. Polini, Quantum versus classical many-body batteries, *Phys. Rev. B* **99**, 205437 (2019).
- [5] J.-Y. Gyhm, D. Šafránek, and D. Rosa, Quantum charging advantage cannot be extensive without global operations, *Phys. Rev. Lett.* **128**, 140501 (2022).
- [6] D. Rossini, G. M. Andolina, D. Rosa, M. Carrega, and M. Polini, Quantum advantage in the charging process of Sachdev-Ye-Kitaev batteries, *Phys. Rev. Lett.* **125**, 236402 (2020).
- [7] S. Seah, M. Perarnau-Llobet, G. Haack, N. Brunner, and S. Nimmrichter, Quantum speed-up in collisional battery charging, *Phys. Rev. Lett.* **127**, 100601 (2021).
- [8] F. Campaioli, F. A. Pollock, F. C. Binder, L. Céleri, J. Goold, S. Vinjanampathy, and K. Modi, Enhancing the charging power of quantum batteries, *Phys. Rev. Lett.* **118**, 150601 (2017).
- [9] F.-Q. Dou, Y.-Q. Lu, Y.-J. Wang, and J.-A. Sun, Extended Dicke quantum battery with interatomic interactions and driving field, *Phys. Rev. B* **105**, 115405 (2022).
- [10] L. Peng, W.-B. He, S. Chesi, H.-Q. Lin, and X.-W. Guan, Lower and upper bounds of quantum battery power in multiple central spin systems, *Phys. Rev. A* **103**, 052220 (2021).
- [11] F. Mayo and A. J. Roncaglia, Collective effects and quantum coherence in dissipative charging of quantum batteries, *Phys. Rev. A* **105**, 062203 (2022).
- [12] F.-Q. Dou, H. Zhou, and J.-A. Sun, Cavity Heisenberg-spin-chain quantum battery, *Phys. Rev. A* **106**, 032212 (2022).
- [13] A. C. Santos, Quantum advantage of two-level batteries in the self-discharging process, *Phys. Rev. E* **103**, 042118 (2021).
- [14] T. P. Le, J. Levinsen, K. Modi, M. M. Parish, and F. A. Pollock, Spin-chain model of a many-body quantum battery, *Phys. Rev. A* **97**, 022106 (2018).
- [15] S.-F. Qi and J. Jing, Magnon-mediated quantum battery under systematic errors, *Phys. Rev. A* **104**, 032606 (2021).
- [16] A. C. Santos, B. Çakmak, S. Campbell, and N. T. Zinner, Stable adiabatic quantum batteries, *Phys. Rev. E* **100**, 032107 (2019).
- [17] A. Rojo-Francàs, F. Isaule, A. C. Santos, B. Juliá-Díaz, and N. T. Zinner, Stable collective charging of ultracold-atom quantum batteries, *Phys. Rev. A* **110**, 032205 (2024).
- [18] D.-L. Yang, F.-M. Yang, and F.-Q. Dou, Three-level Dicke quantum battery, *Phys. Rev. B* **109**, 235432 (2024).
- [19] V. Shaghghi, V. Singh, G. Benenti, and D. Rosa, Micromasers as quantum batteries, *Quantum Sci. Technol.* **7**, 04LT01 (2022).
- [20] B. Ahmadi, P. Mazurek, P. Horodecki, and S. Barzanjeh, Nonreciprocal quantum batteries, *Phys. Rev. Lett.* **132**, 210402 (2024).
- [21] F. Zhao, F.-Q. Dou, and Q. Zhao, Charging performance of the Su-Schrieffer-Heeger quantum battery, *Phys. Rev. Res.* **4**, 013172 (2022).
- [22] F.-M. Yang and F.-Q. Dou, Wireless energy transfer in a non-Hermitian quantum battery, *Phys. Rev. A* **112**, 042205 (2025).
- [23] Y. Kurman, K. Hymas, A. Fedorov, W. J. Munro, and J. Quach, Powering quantum computation with quantum batteries, *Phys. Rev. X* **16**, 011016 (2026).
- [24] Z.-G. Lu, G. Tian, X.-Y. Lü, and C. Shang, Topological quantum batteries, *Phys. Rev. Lett.* **134**, 180401 (2025).
- [25] F. Pirmoradian and K. Mølmer, Aging of a quantum battery, *Phys. Rev. A* **100**, 043833 (2019).
- [26] J. Monsel, M. Fellous-Asiani, B. Huard, and A. Auffèves, The energetic cost of work extraction, *Phys. Rev. Lett.* **124**, 130601 (2020).
- [27] F.-Q. Dou and F.-M. Yang, Superconducting transmon qubit-resonator quantum battery, *Phys. Rev. A* **107**, 023725 (2023).
- [28] F. T. Tabesh, F. H. Kamin, and S. Salimi, Environment-mediated charging process of quantum batteries, *Phys. Rev. A* **102**, 052223 (2020).
- [29] W.-L. Song, H.-B. Liu, B. Zhou, W.-L. Yang, and J.-H. An, Remote charging and degradation suppression for the quantum battery, *Phys. Rev. Lett.* **132**, 090401 (2024).
- [30] F. Barra, Dissipative charging of a quantum battery, *Phys. Rev. Lett.* **122**, 210601 (2019).
- [31] F.-M. Yang and F.-Q. Dou, Resonator-qutrit quantum battery, *Phys. Rev. A* **109**, 062432 (2024).
- [32] F. Zhao, F.-Q. Dou, and Q. Zhao, Quantum battery of interacting spins with environmental noise, *Phys. Rev. A* **103**, 033715 (2021).
- [33] S. Tirone, R. Salvia, S. Chessa, and V. Giovannetti, Work extraction processes from noisy quantum batteries: The role of nonlocal resources, *Phys. Rev. Lett.* **131**, 060402 (2023).
- [34] R. Grazi, D. Sacco Shaikh, M. Sassetti, N. Traverso Ziani, and D. Ferraro, Controlling energy storage crossing quantum phase transitions in an integrable spin quantum battery, *Phys. Rev. Lett.* **133**, 197001 (2024).
- [35] P.-Y. Sun, H. Zhou, and F.-Q. Dou, Cavity-Heisenberg spin-j chain quantum battery and reinforcement learning optimization, *New J. Phys.* **27**, 124513 (2025).
- [36] R. P. A. Simon, J. Anders, and K. V. Hovhannisyán, Correlations enable lossless ergotropy transport, *Phys. Rev. Lett.* **134**, 010408 (2025).
- [37] I. Medina, O. Culhane, F. C. Binder, G. T. Landi, and J. Goold, Anomalous discharging of quantum batteries:

- The ergotropic Mpemba effect, *Phys. Rev. Lett.* **134**, 220402 (2025).
- [38] L. Wang, S.-Q. Liu, F.-l. Wu, H. Fan, N.-N. Li, and S.-Y. Liu, Global and local performance of a quantum battery under correlated noise channels, *Phys. Rev. A* **112**, 022206 (2025).
- [39] S.-Y. Bai and J.-H. An, Floquet engineering to reactivate a dissipative quantum battery, *Phys. Rev. A* **102**, 060201 (2020).
- [40] J. Q. Quach, K. E. McGhee, L. Ganzer, D. M. Rouse, B. W. Lovett, E. M. Gauger, J. Keeling, G. Cerullo, D. G. Lidzey, and T. Virgili, Superabsorption in an organic microcavity: Toward a quantum battery, *Sci. Adv.* **8**, eabk3160 (2022).
- [41] J. Joshi and T. S. Mahesh, Experimental investigation of a quantum battery using star-topology NMR spin systems, *Phys. Rev. A* **106**, 042601 (2022).
- [42] I. Maillette de Buy Wenniger, S. E. Thomas, M. Maffei, S. C. Wein, M. Pont, N. Belabas, S. Prasad, A. Harouri, A. Lemaitre, I. Sagnes, N. Somaschi, A. Auffèves, and P. Senellart, Experimental analysis of energy transfers between a quantum emitter and light fields, *Phys. Rev. Lett.* **131**, 260401 (2023).
- [43] X. Huang, K. Wang, L. Xiao, L. Gao, H. Lin, and P. Xue, Demonstration of the charging progress of quantum batteries, *Phys. Rev. A* **107**, L030201 (2023).
- [44] C.-K. Hu, J. Qiu, P. J. P. Souza, J. Yuan, Y. Zhou, L. Zhang, J. Chu, X. Pan, L. Hu, J. Li, Y. Xu, Y. Zhong, S. Liu, F. Yan, D. Tan, R. Bachelard, C. J. Villas-Boas, A. C. Santos, and D. Yu, Optimal charging of a superconducting quantum battery, *Quantum Sci. Technol.* **7**, 045018 (2022).
- [45] R.-H. Zheng, W. Ning, Z.-B. Yang, Y. Xia, and S.-B. Zheng, Demonstration of dynamical control of three-level open systems with a superconducting qutrit, *New J. Phys.* **24**, 063031 (2022).
- [46] G. Zhu, Y. Chen, Y. Hasegawa, and P. Xue, Charging quantum batteries via indefinite causal order: Theory and experiment, *Phys. Rev. Lett.* **131**, 240401 (2023).
- [47] C.-K. Hu, C. Liu, J. Zhao, L. Zhong, Y. Zhou, M. Liu, H. Yuan, Y. Lin, Y. Xu, G. Hu, G. Xie, Z. Liu, R. Zhou, Y. Ri, W. Zhang, R. Deng, A. Saguia, X. Linpeng, M. S. Sarandy, S. Liu, A. C. Santos, D. Tan, and D. Yu, Quantum charging advantage in superconducting solid-state batteries, *Phys. Rev. Lett.* **136**, 060401 (2026).
- [48] L. Li, S.-L. Zhao, Y.-H. Shi, B.-J. Chen, X. Ruan, G.-H. Liang, W.-P. Yuan, J.-C. Song, C.-L. Deng, Y. Liu, T.-M. Li, Z.-H. Liu, X.-Y. Guo, X. Song, K. Xu, H. Fan, Z. Xiang, and D. Zheng, Stable and efficient charging of superconducting capacitively shunted flux quantum batteries, *Phys. Rev. Appl.* **24**, 054033 (2025).
- [49] D. Ferraro, M. Campisi, G. M. Andolina, V. Pellegrini, and M. Polini, High-power collective charging of a solid-state quantum battery, *Phys. Rev. Lett.* **120**, 117702 (2018).
- [50] P. Forn-Díaz, L. Lamata, E. Rico, J. Kono, and E. Solano, Ultrastrong coupling regimes of light-matter interaction, *Rev. Mod. Phys.* **91**, 025005 (2019).
- [51] W. T. M. Irvine, K. Hennessy, and D. Bouwmeester, Strong coupling between single photons in semiconductor microcavities, *Phys. Rev. Lett.* **96**, 057405 (2006).
- [52] A. Wallraff, D. I. Schuster, A. Blais, L. Frunzio, R.-. S. Huang, J. Majer, S. Kumar, S. M. Girvin, and R. J. Schoelkopf, Strong coupling of a single photon to a superconducting qubit using circuit quantum electrodynamics, *Nature* **431**, 162 (2004).
- [53] A. Stockklauser, P. Scarlino, J. V. Koski, S. Gasparinetti, C. K. Andersen, C. Reichl, W. Wegscheider, T. Ihn, K. Ensslin, and A. Wallraff, Strong coupling cavity QED with gate-defined double quantum dots enabled by a high impedance resonator, *Phys. Rev. X* **7**, 011030 (2017).
- [54] D. I. Schuster, A. P. Sears, E. Ginossar, L. DiCarlo, L. Frunzio, J. J. L. Morton, H. Wu, G. A. D. Briggs, B. B. Buckley, D. D. Awschalom, and R. J. Schoelkopf, High-cooperativity coupling of electron-spin ensembles to superconducting cavities, *Phys. Rev. Lett.* **105**, 140501 (2010).
- [55] Y. Kubo, F. R. Ong, P. Bertet, D. Vion, V. Jacques, D. Zheng, A. Dréau, J.-F. Roch, A. Auffèves, F. Jelezko, J. Wrachtrup, M. F. Barthe, P. Bergonzo, and D. Esteve, Strong coupling of a spin ensemble to a superconducting resonator, *Phys. Rev. Lett.* **105**, 140502 (2010).
- [56] K. D. Petersson, L. W. McFaul, M. D. Schroer, M. Jung, J. M. Taylor, A. A. Houck, and J. R. Petta, Circuit quantum electrodynamics with a spin qubit, *Nature* **490**, 380 (2012).
- [57] F. Yoshihara, T. Fuse, S. Ashhab, K. Kakuyanagi, S. Saito, and K. Semba, Superconducting qubit-oscillator circuit beyond the ultrastrong-coupling regime, *Nat. Phys.* **13**, 44 (2017).
- [58] P. Forn-Díaz, J. J. García-Ripoll, B. Peropadre, J.-L. Orgiazzi, M. A. Yurtalan, R. Belyansky, C. M. Wilson, and A. Lupascu, Ultrastrong coupling of a single artificial atom to an electromagnetic continuum in the nonperturbative regime, *Nat. Phys.* **13**, 39 (2017).
- [59] N. Gheeraert, S. Bera, and S. Florens, Spontaneous emission of schrödinger cats in a waveguide at ultrastrong coupling, *New J. Phys.* **19**, 023036 (2017).
- [60] D. Ballester, G. Romero, J. J. García-Ripoll, F. Deppe, and E. Solano, Quantum simulation of the ultrastrong-coupling dynamics in circuit quantum electrodynamics, *Phys. Rev. X* **2**, 021007 (2012).
- [61] G. Günter, A. A. Anappara, J. Hees, A. Sell, G. Biasiol, L. Sorba, S. De Liberato, C. Ciuti, A. Tredicucci, A. Leitenstorfer, and R. Huber, Sub-cycle switch-on of ultrastrong light-matter interaction, *Nature* **458**, 178 (2009).
- [62] T. Niemczyk, F. Deppe, H. Huebl, E. P. Menzel, F. Hocke, M. J. Schwarz, J. J. Garcia-Ripoll, D. Zueco, T. Hümmer, E. Solano, A. Marx, and R. Gross, Circuit quantum electrodynamics in the ultrastrong-coupling regime, *Nat. Phys.* **6**, 772 (2010).
- [63] N. K. Langford, R. Sagastizabal, M. Kounalakis, C. Dickel, A. Bruno, F. Luthi, D. J. Thoen, A. Endo, and L. DiCarlo, Experimentally simulating the dynamics of quantum light and matter at deep-strong coupling, *Nat. Commun.* **8**, 1715 (2017).
- [64] J. Casanova, G. Romero, I. Lizuain, J. J. García-Ripoll, and E. Solano, Deep strong coupling regime of the Jaynes-Cummings model, *Phys. Rev. Lett.* **105**, 263603 (2010).
- [65] D. Z. Rossatto, C. J. Villas-Bôas, M. Sanz, and E. Solano, Spectral classification of coupling regimes in the quantum Rabi model, *Phys. Rev. A* **96**, 013849 (2017).
- [66] A. A. Anappara, S. De Liberato, A. Tredicucci, C. Ciuti, G. Biasiol, L. Sorba, and F. Beltram, Signatures of the

- ultrastrong light-matter coupling regime, *Phys. Rev. B* **79**, 201303 (2009).
- [67] P. Forn-Díaz, J. Lisenfeld, D. Marcos, J. J. García-Ripoll, E. Solano, C. J. P. M. Harmans, and J. E. Mooij, Observation of the Bloch-Siegert shift in a qubit-oscillator system in the ultrastrong coupling regime, *Phys. Rev. Lett.* **105**, 237001 (2010).
- [68] P. Nataf and C. Ciuti, Protected quantum computation with multiple resonators in ultrastrong coupling circuit QED, *Phys. Rev. Lett.* **107**, 190402 (2011).
- [69] G. Romero, D. Ballester, Y. M. Wang, V. Scarani, and E. Solano, Ultrafast quantum gates in circuit QED, *Phys. Rev. Lett.* **108**, 120501 (2012).
- [70] Y. Wang, J. Zhang, C. Wu, J. Q. You, and G. Romero, Holonomic quantum computation in the ultrastrong-coupling regime of circuit QED, *Phys. Rev. A* **94**, 012328 (2016).
- [71] F. Armata, G. Calajo, T. Jaako, M. S. Kim, and P. Rabl, Harvesting multiqubit entanglement from ultrastrong interactions in circuit quantum electrodynamics, *Phys. Rev. Lett.* **119**, 183602 (2017).
- [72] A. de la Torre, D. M. Kennes, M. Claassen, S. Gerber, J. W. McIver, and M. A. Sentef, Colloquium: Nonthermal pathways to ultrafast control in quantum materials, *Rev. Mod. Phys.* **93**, 041002 (2021).
- [73] P. D. Nation, J. R. Johansson, M. P. Blencowe, and F. Nori, Colloquium: Stimulating uncertainty: Amplifying the quantum vacuum with superconducting circuits, *Rev. Mod. Phys.* **84**, 1 (2012).
- [74] X.-Y. Lü, Y. Wu, J. R. Johansson, H. Jing, J. Zhang, and F. Nori, Squeezed optomechanics with phase-matched amplification and dissipation, *Phys. Rev. Lett.* **114**, 093602 (2015).
- [75] I. Siddiqi, R. Vijay, F. Pierre, C. M. Wilson, M. Metcalfe, C. Rigetti, L. Frunzio, and M. H. Devoret, Rf-driven Josephson bifurcation amplifier for quantum measurement, *Phys. Rev. Lett.* **93**, 207002 (2004).
- [76] M.-A. Lemonde, N. Didier, and A. A. Clerk, Enhanced nonlinear interactions in quantum optomechanics via mechanical amplification, *Nat. Commun.* **7**, 11338 (2016).
- [77] D. M. Long, P. J. D. Crowley, A. J. Kollár, and A. Chandran, Boosting the quantum state of a cavity with Floquet driving, *Phys. Rev. Lett.* **128**, 183602 (2022).
- [78] P. Groszkowski, H.-K. Lau, C. Leroux, L. C. G. Govia, and A. A. Clerk, Heisenberg-limited spin squeezing via bosonic parametric driving, *Phys. Rev. Lett.* **125**, 203601 (2020).
- [79] C. Leroux, L. C. G. Govia, and A. A. Clerk, Enhancing cavity quantum electrodynamics via antisqueezing: Synthetic ultrastrong coupling, *Phys. Rev. Lett.* **120**, 093602 (2018).
- [80] L.-X. Guo, L.-L. Wan, L.-G. Si, and Y. Wu, Topological amplification and frequency conversion in a photonic lattice with a two-photon driving, *Phys. Rev. A* **108**, 013512 (2023).
- [81] S.-Y. Guan, H.-F. Wang, and X. Yi, Manipulation of tunable nonreciprocal entanglement and one-way steering induced by two-photon driving, *Phys. Rev. A* **109**, 062423 (2024).
- [82] N. Bartolo, F. Minganti, W. Casteels, and C. Ciuti, Exact steady state of a Kerr resonator with one- and two-photon driving and dissipation: Controllable Wigner-function multimodality and dissipative phase transitions, *Phys. Rev. A* **94**, 033841 (2016).
- [83] D. M. Toyli, A. W. Eddins, S. Boutin, S. Puri, D. Hover, V. Bolkhovskiy, W. D. Oliver, A. Blais, and I. Siddiqi, Resonance fluorescence from an artificial atom in squeezed vacuum, *Phys. Rev. X* **6**, 031004 (2016).
- [84] Y. Chen, C. Neill, P. Roushan, N. Leung, M. Fang, R. Barends, J. Kelly, B. Campbell, Z. Chen, B. Chiaro, A. Dunsworth, E. Jeffrey, A. Megrant, J. Y. Mutus, P. J. J. O'Malley, C. M. Quintana, D. Sank, A. Vainsencher, J. Wenner, T. C. White, M. R. Geller, A. N. Cleland, and J. M. Martinis, Qubit architecture with high coherence and fast tunable coupling, *Phys. Rev. Lett.* **113**, 220502 (2014).
- [85] J. Koch, T. M. Yu, J. Gambetta, A. A. Houck, D. I. Schuster, J. Majer, A. Blais, M. H. Devoret, S. M. Girvin, and R. J. Schoelkopf, Charge-insensitive qubit design derived from the Cooper pair box, *Phys. Rev. A* **76**, 042319 (2007).
- [86] Y. Zhang, J. C. Curtis, C. S. Wang, R. J. Schoelkopf, and S. M. Girvin, Drive-induced nonlinearities of cavity modes coupled to a transmon ancilla, *Phys. Rev. A* **105**, 022423 (2022).
- [87] P. Bertet, A. Auffeves, P. Maioli, S. Osnaghi, T. Meunier, M. Brune, J. M. Raimond, and S. Haroche, Direct measurement of the Wigner function of a one-photon Fock state in a cavity, *Phys. Rev. Lett.* **89**, 200402 (2002).
- [88] L. F. Buchmann, S. Schreppler, J. Kohler, N. Spethmann, and D. M. Stamper-Kurn, Complex squeezing and force measurement beyond the standard quantum limit, *Phys. Rev. Lett.* **117**, 030801 (2016).
- [89] O. Arcizet, T. Briant, A. Heidmann, and M. Pinard, Beating quantum limits in an optomechanical sensor by cavity detuning, *Phys. Rev. A* **73**, 033819 (2006).
- [90] P. Krantz, M. Kjaergaard, F. Yan, T. P. Orlando, S. Gustavsson, and W. D. Oliver, A quantum engineer's guide to superconducting qubits, *Appl. Phys. Rev.* **6**, 021318 (2019).
- [91] Y.-F. Qiao, J.-H. An, and P.-B. Li, Mechanical squeezed-Fock qubit: Towards quantum weak-force sensing, *Phys. Rev. Lett.* **136**, 040801 (2026).
- [92] A. Crescente, M. Carrega, M. Sassetti, and D. Ferraro, Ultrafast charging in a two-photon Dicke quantum battery, *Phys. Rev. B* **102**, 245407 (2020).
- [93] Z. Wang, H. Li, W. Feng, X. Song, C. Song, W. Liu, Q. Guo, X. Zhang, H. Dong, D. Zheng, H. Wang, and D.-W. Wang, Controllable switching between superradiant and subradiant states in a 10-qubit superconducting circuit, *Phys. Rev. Lett.* **124**, 013601 (2020).
- [94] M. Zanner, T. Orell, C. M. F. Schneider, R. Albert, S. Oleschko, M. L. Juan, M. Silveri, and G. Kirchmair, Coherent control of a multi-qubit dark state in waveguide quantum electrodynamics, *Nat. Phys.* **18**, 538 (2022).
- [95] J. Q. Quach and W. J. Munro, Using dark states to charge and stabilize open quantum batteries, *Phys. Rev. Appl.* **14**, 024092 (2020).
- [96] C. Emary and T. Brandes, Chaos and the quantum phase transition in the Dicke model, *Phys. Rev. E* **67**, 066203 (2003).
- [97] C. J. Zhu, L. L. Ping, Y. P. Yang, and G. S. Agarwal, Squeezed light induced symmetry breaking superradiant phase transition, *Phys. Rev. Lett.* **124**, 073602 (2020).
- [98] D. Novokreschenov, A. Kudlis, I. Iorsh, and I. V.

- Tokatly, Quantum electrodynamical density functional theory for generalized Dicke model, [Phys. Rev. B **108**, 235424 \(2023\)](#).
- [99] K. Baumann, R. Mottl, F. Brennecke, and T. Esslinger, Exploring symmetry breaking at the Dicke quantum phase transition, [Phys. Rev. Lett. **107**, 140402 \(2011\)](#).
- [100] A. Blais, R.-S. Huang, A. Wallraff, S. M. Girvin, and R. J. Schoelkopf, Cavity quantum electrodynamics for superconducting electrical circuits: An architecture for quantum computation, [Phys. Rev. A **69**, 062320 \(2004\)](#).
- [101] A. Blais, A. L. Grimsmo, S. M. Girvin, and A. Wallraff, Circuit quantum electrodynamics, [Rev. Mod. Phys. **93**, 025005 \(2021\)](#).
- [102] L. P. García-Pintos, A. Hamma, and A. del Campo, Fluctuations in extractable work bound the charging power of quantum batteries, [Phys. Rev. Lett. **125**, 040601 \(2020\)](#).